Desalination and Water Treatment
www.deswater.com
doi: 10.1080/19443994.2014.946711

55 (2015) 2777–2785
August

Productivity analysis of two spiral-wound membrane distillation prototypes coupled with solar energy

Alba Ruiz-Aguirre[a], Diego-César Alarcón-Padilla[b], Guillermo Zaragoza[b,*]

[a]*Universidad de Almería – CIESOL, Ctra. Sacramento s/n, La Cañada de San Urbano, Almería 04120 Spain, email: alba.ruiz@psa.es (A. Ruiz-Aguirre)*
[b]*CIEMAT-Plataforma Solar de Almería, Ctra. de Senés s/n, Almería, 04200 Tabernas, Spain, email: diego.alarcon@psa.es (D.-C. Alarcón-Padilla), Tel. +34 950387800; email: guillermo.zaragoza@psa.es (G. Zaragoza)*

Received 7 April 2014; Accepted 16 June 2014

ABSTRACT

The use of solar energy to feed the MD desalination process is being evaluated at Plataforma Solar de Almería, the largest European facility for solar energy research, located in SE Spain. A test bed for the evaluation of membrane distillation modules is under operation coupled to a field of static solar collectors. Different commercial modules and real-scale prototypes are tested in continuous operation and coupled with a solar thermal source, in order to obtain data in conditions closer to real applications than the tests performed at laboratory scale. This particular study shows an evaluation of two different modules using spiral-wound membranes, one with a liquid-gap configuration (built by Solar Spring) and the other with an air-gap configuration (built by Aquastill). An assessment of the influence of the operational parameters in the performance was done within the allowed ranges of operation of each prototype, with special attention to the temperatures and the feed flow rate. Also, the influence of the salinity was investigated using feed water with salts at different values of conductivity. The characterization of the systems is done based on the quality of the distillate, as well as the measured values of distillate production and thermal performance, choosing the specific distillate flux obtained and the gain output ratio (GOR) as performance indicators. The main results of the analysis are summarized and compared, discussing the particular operational experiences in each case.

Keywords: Solar desalination; Membrane distillation; Experimental results; Renewable energy desalination

1. Introduction

The water crisis is a global problem. In the last century, water use has surpassed the sustainability level in an increasing number of regions. Nearly, 1,200 million people live in regions with physical water scarcity while 1,600 million have economic water scarcity [1]. The regions most affected by the scarcity of freshwater have arid and semi-arid climates. In order to meet the demand in these areas, desalination processes are considered a suitable proposal. However, conventional desalination technologies such as multi-stage flash

*Corresponding author.

Presented at the Conference on Desalination for the Environment: Clean Water and Energy 11–15 May 2014, Limassol, Cyprus

distillation (MSF), multi-effect distillation (MED) or reverse osmosis (RO) are not always a good choice, because they are designed for industrial-scale water production and plenty of these zones require a small production of water. This creates the necessity of developing medium size, robust and autonomous desalination units using alternative energy sources [2]. While it is true that RO can be downscaled and fed with photovoltaic energy, the complications derived from its discontinuous operation require skilled technicians which are not always available in these places. On the other hand, solar membrane distillation (SMD) can adapt better to discontinuous operation and has the potential to become a suitable and sustainable solution to put an end to the water deficit in these areas which receive high solar irradiation for many hours per day.

Membrane distillation (MD) is a non-isothermal membrane separation process known since the 1960s. However, until the 1980s, commercial membranes with the desired properties were not available. The driving force of the process is the vapour pressure difference created by a temperature difference between both sides of a hydrophobic microporous membrane. Only vapour is transported through the membrane due to the liquid-rejecting properties of the membrane materials. However, the liquid phase can penetrate the pores if the hydrostatic pressure exceeds the minimum liquid entry pressure (LEP). So, membranes for MD must have a high LEP to prevent the passage of liquid. Besides, a low resistance to mass transfer is required to help the vapour flux, and a low thermal conductivity is desirable to minimize heat losses and maintain the necessary temperature gradient. In comparison with other membrane separation processes, MD is not driven by absolute pressure, which has several advantages. On the one hand, the size of the pores can be larger (from 0.2 to 1 μm [3]). This fact, together with the hydrophobicity of the membrane, decreases the risk of clogging, which eliminates the need of chemical pre-treatment to water before entering the modules, just a simple pre-filtration would be necessary. On the other hand, water with a high concentration of solutes can be treated. This is the case of water with high salinity which increases the energy consumption and membrane fouling in a RO treatment, like concentrated brines or even sea water from the Arabian Gulf [4]. Since MD is an evaporative process, a complete rejection of non-volatile compound occurs and the quality of the distillate is independent of the feed water. Furthermore, the range of operating temperatures enables the use of waste heat and renewable energy sources such as solar thermal.

The driving force of the MD process can be set up with five different module configurations [5,6]. The most simple configuration is direct contact membrane distillation (DCMD), in which a solution cooler than the feed is in direct contact with the permeate side of the membrane. Evaporation of the volatile molecules takes place in the hot liquid–vapour interface due to the vapour pressure difference generated by the trans-membrane temperature difference. Then, vapour crosses the pore of the membrane and condenses in the cold liquid/vapour interface created in the permeate side. Therefore, in this configuration, the distillate produced is mixed with the cold solution. The main drawback of this MD configuration is the large sensible heat losses by conduction through the membrane. To reduce them, a condensation surface is introduced in the module, separated from the membrane by a layer of stagnant air. This configuration is called air-gap membrane distillation (AGMD). The coolant solution circulates through the other side of the condensation surface, and vapour crosses the air gap to condense over the cold surface. Because of the air gap, there is an additional mass transfer resistance and therefore, the distillate fluxes obtained are lower. This disadvantage can be remedied if the gap is full of a stagnant cold liquid that usually is the distillate. This configuration, liquid-gap membrane distillation (LGMD), has fewer heat losses by conduction than DCMD, and the mass transfer resistance is lower than in AGMD. Besides the previous configurations, there are two more in which the condensation takes place outside the module in a separate unit. In sweeping gas membrane distillation (SGMD), cold inert gas sweeps the vapour from the permeate side to the condenser. To avoid the subsequent separation of vapour and gas, a vacuum can be applied in the permeate side. This reduces the conductive heat losses, but with the vacuum, the LEP of the membrane pores can be surpassed causing membrane wetting.

MD can be used for different purposes apart from desalination, such as concentration of ions, colloids or other non-volatile compounds from aqueous dilutions, and removal of non-volatile pollutants and micro-organism from wastewater. MD has been extensively studied at small scale; however, further experimentation at a higher scale is necessary for its complete industrial development and usually the results obtained at pilot scale do not match with the ones achieved at a laboratory scale [7].

In order to assess the technology of membrane distillation under real conditions and coupled with solar energy, two test beds have been built at Plataforma Solar de Almería (PSA) (SE Spain). Several prototypes have been analysed. This study shows a preliminary evaluation of two different modules using spiral-wound membranes, one with a liquid-gap configuration and the other with an air-gap configuration.

2. Materials and methods

The experiments were performed at Plataforma Solar of Almería during several months of operation with real solar energy conditions, using static solar thermal collectors at about 85˚C. The test beds have been described elsewhere [7]. Two full-scale MD commercial units with spiral wound modules have been evaluated. One is the Oryx 150 unit built by the German company Solar Spring GmbH [8] and the other a pilot unit by Dutch company Aquastill. The former uses a LGMD configuration, while the latter is AGMD.

2.1. Spiral wound modules

The use of spiral-wound modules in MD came up more than 20 years ago [9,10]. In this type of modules (Fig. 1), flat sheet membranes, channels and spacers are assembled and rolled around a tube. This way, the membrane reaches a packing density between 300 m^2/m^3 and 1,000 m^2/m^3, reducing the space occupation.

Modules with AGMD and LGMD configuration comprise three channels: the evaporator channel, the cooling channel and the distillate channel, which is between the former two. Feed water is pumped into the cooling channel. In this channel, the temperature of the water is increased by the internal heat recovery and then it flows through a heat exchanger to further raise its temperature. The heat exchanger receives heat from an external heat source; in this case, a field of static solar collectors. Then, the hot water flows through the evaporator channel in counter-current flow with water from the cooling channel. In this channel, evaporation takes place, vapour passes through the membrane and the remaining brine is returned to the feed tank. The vapour condenses on the condenser foil, and in the AGMD, it slides down to be collected at the bottom of the module, while in the LGMD, it remains in the gap and overflows at the top of the module. Latent heat of condensation is recovered as sensible heat to increase the temperature of the feed while acting as coolant and minimize the external heat supply. The spiral-wound configuration and the counter-current flow of the coolant and the hot water maximize internal heat recovery. Fig. 2 shows a diagram of the solar MD experimental unit.

The Oryx 150 unit by Solar Spring uses a module with a LGMD configuration developed in collaboration with the Fraunhofer Institute [8]. The module is 900 mm high and has a diameter of 360 mm and all the connections (inlets and outlets of the cold and hot streams and distillate outlet) are located in the upper part of the module (Fig. 3). The AGMD Aquastill module has a height of 500 mm and a diameter of 600 mm, with the distillate outlet located at the bottom of the module, as the brine outlet and the feed water inlet, while the outlet of the cooling channel and the inlet of the evaporator channel are on the top side (Fig. 4).

The membrane of the Solar Spring module is made of PTFE, a hydrophobic polymer which has a low surface energy and an exceptional chemical resistance together with a good thermal stability [12]. However, in the Aquastill module, the membrane used is a special kind of PE. The membrane used by Solar Spring has an effective area of 10 m^2 and a length of 7 m, with nominal pore size of 0.2 μm, porosity of 80% and thickness of 70 μm. The rest of the module components are manufactured of plastic too, such as ETFE for the condenser foil, LDPE for the spacers and GFK in the case of the shell [13]. The membrane used by

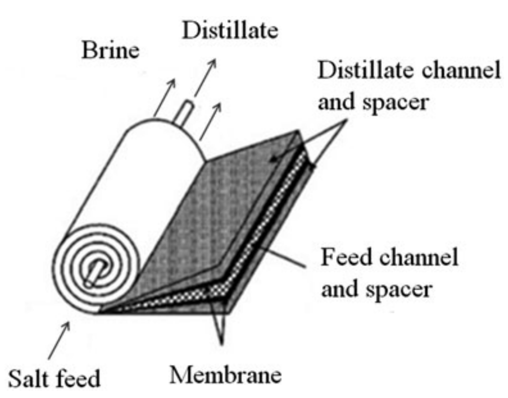

Fig. 1. Schematic diagram of a spiral-wound module (adapted from [11]).

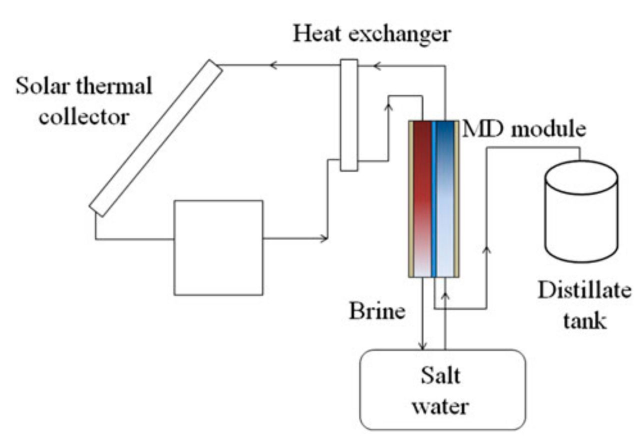

Fig. 2. Schematic diagram of the solar MD experimental unit.

Fig. 3. Oryx 150 system at the facilities of PSA.

Aquastill has an effective area of 24 m^2 with a length of 5 m, it has nominal pore size of 0.3 μm, porosity of 85% and thickness of 76 μm. The materials used for the condenser foil, the spacers and the shell are PET-AL-PET, PP and polyurethane, respectively [Aquastill, private communication].

2.2. Performance parameters evaluated in the study

The production of distillate was studied by analysing the distillate flux, calculated as the mass flow rate of distillate produced ($\dot{m}_d$) per unit of surface of membrane.

$$\text{Distillate flux}\left(\frac{l}{h\cdot m^2}\right) = \frac{\dot{m}_d}{\rho_d\cdot \text{specific surface area}} \tag{1}$$

Another important parameter in MD is the recovery ratio (RR), which indicates the fraction of the feed water that is transformed into distillate.

$$\text{RR}(\%) = \frac{\dot{m}_d}{\dot{m}_f}\cdot 100 \tag{2}$$

where $\dot{m}_f$ is the mass flow rate of feed water (kg/s).

The energy efficiency of the system was calculated using the performance parameter gain output ratio (GOR) that is defined as the latent heat necessary to evaporate all the mass flow rate of distillate produced compared with the external heat added [14].

Fig. 4. Aquastill pilot unit at the facilities of PSA.

$$\text{GOR} = \frac{\dot{m}_d\cdot \Delta h_v}{\dot{Q}} \tag{3}$$

where Δh_v is the enthalpy of vaporization (kJ/kg) and $\dot{Q}$ is the rate of thermal energy supplied to the system (kJ/s).

Finally, the quality of the distillate was evaluated by measuring its conductivity and calculating the salt rejection factor:

$$\text{SRF}\,(\%) = \frac{\sigma_f - \sigma_d}{\sigma_f}\cdot 100 \tag{4}$$

where σ_f is the conductivity of the feed and σ_d is the conductivity of the distillate.

2.3. Experimental plan

In MD, the maximum temperature in the evaporator channel is limited by the thermal resistance of the materials (the membrane, usually) to values below 85˚C. So, the maximum operational temperature considered in this study was 80˚C. Modules were operated inside the recommended feed flow rates of each fabricant, in order to avoid surpassing the LEP of the membrane, which would produce unwanted pore wetting, and to guarantee a good internal heat recovery. Experiments were carried out for two different feed flow rates (400 and 600 l/h) in the case of Solar Spring module and, at the moment of writing this paper, for a single feed flow rate (550 l/h) in the Aquastill module. For both MD units, tests were done using a solution of marine salts with total salinities around 1 g/l as control test and 35 g/l to simulate the average salinity of seawater. No pretreatment was used in any case. To keep the salinity constant, operation was performed in batch mode, returning the brine and distillate to the feed tank. The Solar Spring unit has an automated system for refilling the feed tank with cooler salt water as its level decreases during the operation. By operating in batch mode, this system is deactivated and as a result, the temperature of the feed tank increased throughout the operation due to the residual heat carried by the brine. In the Aquastill plant, this problem was minimized using a much larger feed tank. Experiments were performed trying to maintain stationary operational conditions. Every experiment lasted at least 60 min, and the first 15 min were discarded in both modules to avoid possible previous fluctuations from the steady conditions. Operational parameters were monitored and controlled by a supervisory control and data acquisition (SCADA) connected through a programmable logic controller (PLC). Measures of feed and distillate conductivities were done manually every 15 min. In the Solar Spring experiments, distillate flow rate was measured every 15 min, so the performance parameters were averaged during 15 min intervals to obtain the corresponding measurement. In the Aquastill experiments, the distillate flow rate was measured with higher frequency, but data were averaged every 15 min for comparison.

3. Results and discussion

The quantity of distillate produced in the two modules was analysed by means of the distillate flux and the recovery ratio. The former is shown in Figs. 5 and 6 for feed salinities 1 and 35 g/l, respectively. Measurements are presented for different values of the temperature difference between the hot inlet and the cold inlet, which is the driving force of the process. For the Solar Spring module data are shown for two different feed flow rates (400 and 600 l/h) and for the Aquastill module, at a feed flow rate of 550 l/h. For all cases, the distillate flux increased with the temperature difference, although it was larger for the Solar Spring module. The increase in productivity with the temperature difference was linear. This is usually the case with real-sized modules, in which macroscopic effects make the productivity trend deviate from Antoine's law which predicts an exponential increase [15]. In the Solar Spring module, an increase

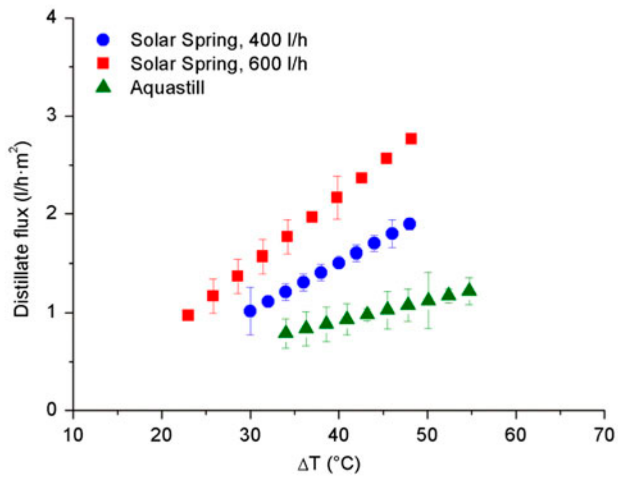

Fig. 5. Variation of the distillate flux with the temperature difference between the hot inlet and the cold inlet for the Solar Spring and Aquastill modules for feed salinity 1 g/l.

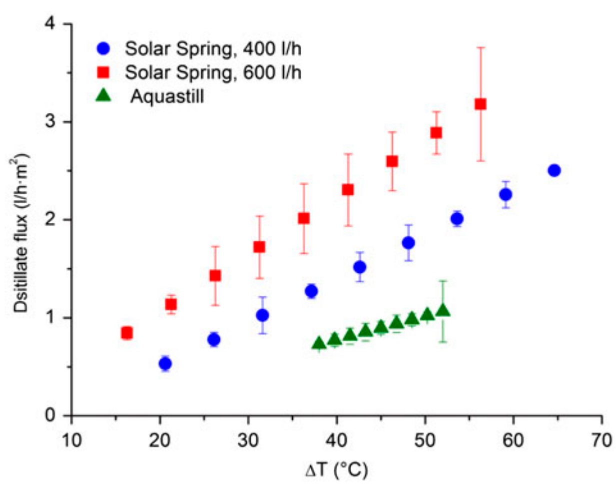

Fig. 6. Variation of the distillate flux with the temperature difference between the hot inlet and the cold inlet for the Solar Spring and Aquastill modules for feed salinity 35 g/l.

in productivity with the feed flow rate was also clear. The influence of salinity was much smaller, and the values obtained for 35 g/l were only slightly lower than for 1 g/l. For instance, the distillate flux obtained with the Solar Spring module at feed salinity 1 g/l was 1.90 l/h m^2 for a temperature difference of 48˚C and a feed flow rate of 400 l/h. For the same conditions, but feed salinity 35 g/l, the measured distillate flux was 1.76 l/h m^2. The distillate flux for the Aquastill module at 550 l/h feed flow rate was lower (by a factor of three for the maximum values) than that for the Solar Spring module at 600 l/h feed flow rate. However, the concentration factors of the saline feed obtained with the Aquastill module were similar or larger than the Solar Spring one. Figs. 7 and 8 show the RR as a function of the temperature difference for both modules and for feed salinities 1 and 35 g/l, respectively. It can be seen that the RR increases linearly with the temperature difference in both modules, with no significant differences between the different feed flow rates in the case of the Solar Spring module. For 1 g/l, and for a temperature difference between 35 and 55˚C, the values obtained for the Aquastill module were slightly larger than the Solar Spring module, though considering the error bars in the data, not significantly. The results for salinity of 35 g/l were similar for all modules, and lower than for feed salinity 1 g/l, especially in the case of the Aquastill module (between 10% and 30% decreases compared with a maximum of 12% in the Solar Spring module).

Efficiency in the use of thermal energy is an important parameter for the industrial implementation of solar thermal desalination. As explained before, GOR was the parameter chosen to assess the thermal energy efficiency. In this study, GOR was calculated for both modules considering only experiments performed at 35 g/l. Fig. 9 shows the values of the GOR obtained for the Solar Spring module at two different feed flow rates, 400 and 600 l/h and for the Aquastill module, a feed flow rate of 550 l/h. The values measured in the Aquastill module were greater than 4 for all cases, reaching values near 7 for the highest temperature difference between the hot inlet and the cold inlet (approximately 50˚C). On the other hand, the GOR measured for the Solar

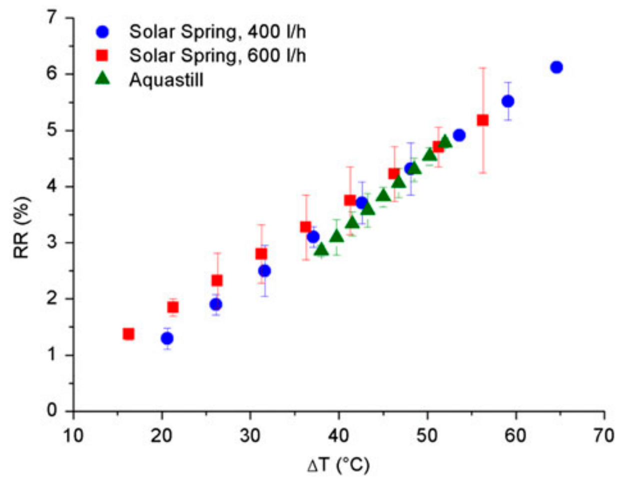

Fig. 8. Variation of the RR with the temperature difference between the hot inlet and the cold inlet for the Solar Spring and Aquastill modules for feed salinity 35 g/l.

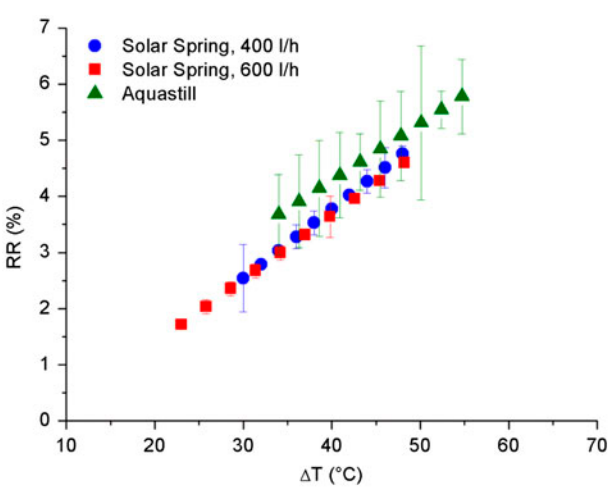

Fig. 7. Variation of the RR with the temperature difference between the hot inlet and the cold inlet for the Solar Spring and Aquastill modules for feed salinity 1 g/l.

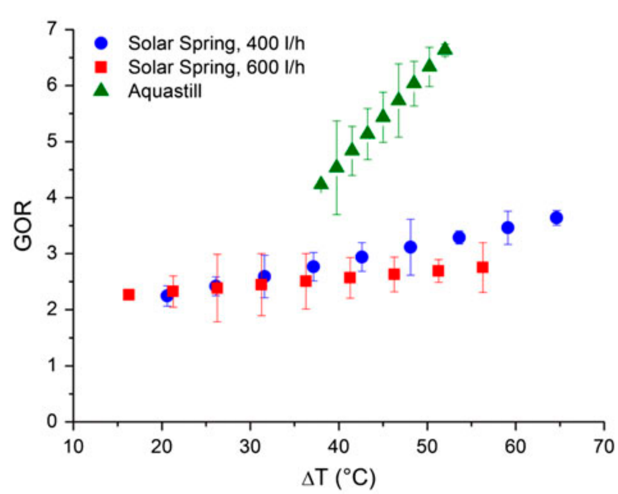

Fig. 9. Variation of the GOR with the temperature difference between the hot inlet and the cold inlet for the Solar Spring and Aquastill modules for feed salinity 35 g/l.

Spring module did not reach 4 even for temperature differences larger than 50℃. These values are significantly larger than those reported for pilot-size plate and frame modules [16]. Moreover, when the feed flow rate was increased in the experiments carried out with the Solar Spring module, the values of GOR decreased. For a temperature differences above 40℃, the values of GOR for the Solar Spring module were higher for 400 g/l feed flow rate, reaching values over 3, while for 600 l/h the maximum value was 2.75. Another significant difference between both modules is the variation of the GOR with the temperature difference. The GOR increased with the temperature difference between the hot side and cold side in both cases, but this effect was greater for the Aquastill module than for the Solar Spring module. For an increase of 14℃ in ΔT, the GOR in Aquastill module increased 57%, while a similar increase in the GOR of the Solar Spring module required a raise in the temperature difference of 40℃ for the case of feed flow rate 400 l/h.

As shown in the results, the temperature difference had a positive effect in all cases; however, the feed flow rate had a different effect in the thermal energy efficiency and the distillate production. This is due to the hydrodynamic conditions being enhanced by achieving a more turbulent regime which decreases polarization effects and therefore favours the flow of vapour. However, turbulence can increase the heat losses across the membrane. Moreover, the different performance of the modules can be related to the different configurations. As aforementioned, the air gap in the AGMD minimizes the heat losses by conduction through the membrane which is responsible for decreasing the thermal efficiency of the MD process. However, the air gap increases the mass transfer resistance, so even though the energy efficiency is higher, the distillate fluxes can be lower. The fact that the effective cross-flow velocity of the Aquastill module is lower than in the Solar Spring module needs also to be taken into account (for feed flow rate of 550 l/h, the effective cross flow velocity in Aquastill is 0.039 m/s while for feed flow rate of 400 l/h in Solar Spring is 0.076 m/s). This means that the contact time of the feed flow with the membrane is larger, which increases the heat recovery. However, the lower effective cross-flow velocity decreases the turbulence and this decreases the vapour flux through the membrane, making the distillate flux lower. Nevertheless, the RR of the Aquastill module is comparable with the Solar Spring one. This means that the total distillate flow rate is not that dissimilar in both modules, since the differences in the feed flow rates are not that large.

3.1. Quality of the distillate

Measured values of distillate conductivity corresponding to feed salinities about 1 and 35 g/l for the Solar Spring module are represented in Fig. 10. For a salinity of 1 g/l, all the results showed excellent distillate quality, always below 20 μS/cm. For a salinity of 35 g/l, the majority of the results showed similar distillate quality (more than half of the measurements between 1 and 5 μS/cm), though the occurrence of very high values (>100 and even >1,000 μS/cm) was remarkable. These correspond to measurements at the beginning of the experiments, and might be explained by salt deposition occurring on the membrane when the process is discontinued [17]. Subsequent flushing of the crystals as more permeate is being produced, which would restore the quality of the distillate. This effect is obviously much less important for a salinity of 1 g/l. Fig. 11 show the measurements of distillate conductivity for salinities 1 and 35 g/l obtained in the

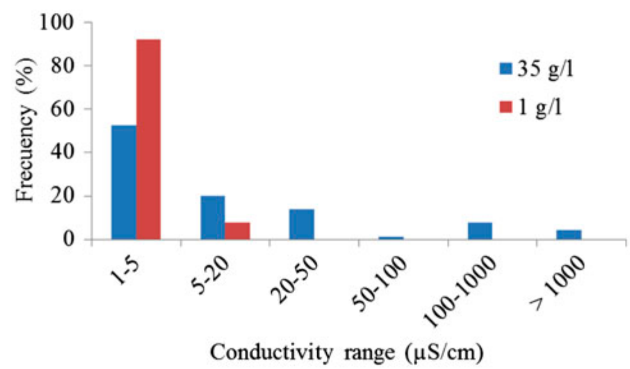

Fig. 10. Frequency distribution of the values of distillate conductivity measured for the Solar Spring module in the experiments carried out with feed salinities 1 and 35 g/l.

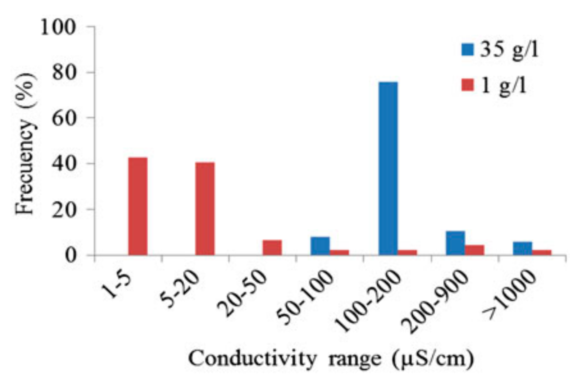

Fig. 11. Frequency distribution of the values of distillate conductivity measured for the Aquastill module in the experiments carried out with feed salinities 1 and 35 g/l.

Aquastill module. If we compare both modules, the measured range of conductivities for a salinity of 1 g/l in the Aquastill module was higher than that in the Solar Spring module, though almost all the measurements fell below 20 μS/cm. Worse results were obtained for a salinity of 35 g/l. In this case, the average conductivities obtained in the Aquastill module were between 100 and 200 μS/cm, much larger than those in Solar Spring module. Figs. 12 and 13 show the salt rejection factor (SRF) for both salinities in the Solar Spring module and Aquastill module, respectively. For 35 g/l feed salinity, salt rejection factors generally greater than 99.9% were achieved in Solar Spring while the maximum SRF obtained in the Aquastill module was 99.9%, and the majority of the values were between 99.6 and 99.8%. These results are concurrent with the larger pore size (and lower hydrophobicity) of the modified PE membrane of the Aquastill module compared with the PTFE membrane of the Solar Spring module.

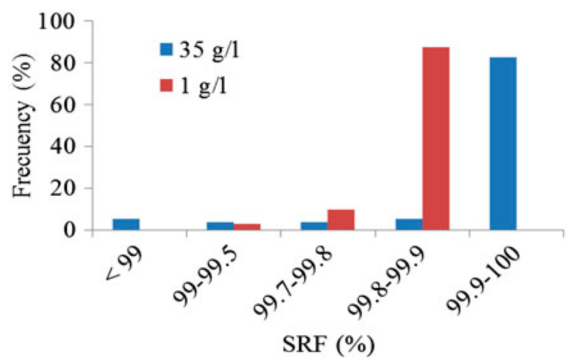

Fig. 12. Frequency distribution of the values of SRF measured for the Solar Spring module in the experiments carried out with feed salinities 1 and 35 g/l.

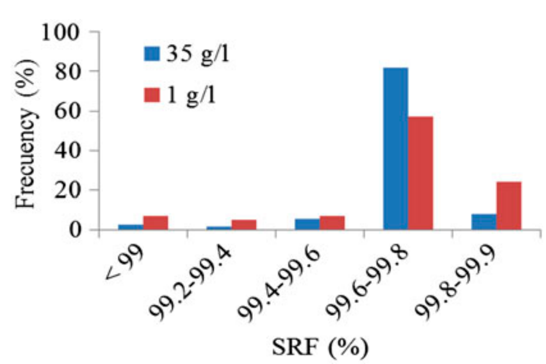

Fig. 13. Frequency distribution of the values of SRF measured for the Aquastill module in the experiments carried out with feed salinities 1 and 35 g/l.

4. Conclusions

Two pilot units of MD developed by different manufacturers using spiral-wound modules are under evaluation for solar desalination at PSA. They are based on two different configurations: one is LGMD (Solar Spring) and the other AGMD (Aquastill). Their performance was analysed and compared for several operational parameters. On one hand, the energy efficiency was larger than in plate and frame modules, with GOR values exceeding 3 in the Solar Spring module and reaching 7 in the Aquastill module. Despite the higher energy efficiency of the latter (GOR about twice higher), distillate fluxes were lower than in the Solar Spring module (even three times smaller). Recovery ratios were similar in both cases. The distillate quality was lower in the Aquastill than in the Solar Spring module, though still acceptable (conductivity values mostly below 200 μS/cm for feed salinity 35 g/l). From this preliminary analysis, it can be concluded that the Aquastill AGMD pilot unit is able to obtain with higher thermal energy efficiency a similar amount of distillate production than the Solar Spring LGMD Oryx 150 unit, using a module with 2.4 larger membrane surface area. The effect of the different membrane characteristics between the two modules need to be studied further before performing an economic analysis.

Acknowledgments

The authors wish to thank the financial support given by the European Commission under the Switch-Asia project Zero Carbon Resorts (reference: 2009/203331).

Abbreviations

MSF	—	multi-stage flash distillation
MED	—	multi-effect distillation
RO	—	reverse osmosis
SMD	—	solar membrane distillation
MD	—	membrane distillation
LEP	—	liquid entry pressure
DCMD	—	direct contact membrane distillation
ACMD	—	air-gap membrane distillation
LGMD	—	liquid-gap membrane distillation
SGMD	—	sweeping-gap membrane distillation
PSA	—	Plataforma Solar de Almería
PTFE	—	polytetrafluoroethylene
PE	—	polyethylene
ETFE	—	ethylene tetrafluoroethylene
LDPE	—	low-density polyethylene
GFK	—	glass reinforced plastic
PET-AL-PET	—	polyethylene terephthalate (aluminium-laminated)

PP	—	polypropylene
SCADA	—	supervisory control and data acquisition
PLC	—	programmable logic controller

Symbols

$\dot{m}$	—	mass flow rate (kg/h)
RR	—	recovery ratio (%)
GOR	—	gain output ratio
Δh_v	—	latent heat of vapourization (kJ/kg)
$\dot{Q}$	—	thermal heat flow rate (kJ/s)
SRF	—	salt rejection factor (%)
σ	—	electrical conductivity (μS/cm)
ΔT	—	temperature difference between hot feed and cold feed of the MD module (°C)
ρ	—	density (kg/l)

Subscripts

d	—	distillate
f	—	feed

References

[1] Coping with water scarcity: Challenge of the Twenty-first Century, UN-Water, FAO, Rome, 2007.
[2] E. Tzen, G. Zaragoza, D.C. Alarcón-Padilla, Solar desalination, in: A. Sayigh (Ed.), Comprehensive Renewable Energy, vol. 3, Elsevier, London, 2012, pp. 529–565.
[3] L.M. Camacho, L. Dumée, J. Zhang, J. Li, M. Duke, J. Gomez, S. Gray, Advances in membrane distillation for water desalination and purification applications, Water 5 (2013) 94–196.
[4] A. Adibfar, The best desalination technology for the Persian Gulf, Int. J. Social Ecol. Sustainable Develop. 2 (4) (2011) 55–65.
[5] A. Alkhudhiri, N. Darwish, N. Hilal, Membrane distillation: A comprehensive review, Desalination 287 (2012) 2–18.
[6] M. Khayet, Membranes and theoretical modeling of membrane distillation: A review, Adv. Colloid Interface Sci. 164 (2011) 56–88.
[7] G. Zaragoza, A. Ruiz-Aguirre, E. Guillén-Burrieza, Efficiency in the use of solar thermal energy of small membrane desalination systems for decentralized water production, Appl. Eng. 130 (2014) 491–499.
[8] J. Koschikowski, M. Wieghaus, M. Rommela, V. Subiela Ortin, B. Peñate Suarez, J.R. Betancort Rodríguez, Experimental investigations on solar driven stand-alone membrane distillation systems for remote areas, Desalination, 248 (2009) 125–131.
[9] D.W. Gore. Gore-Tex membrane distillation, in: Proceedings of the 10th Annual Convention of the Water Supply Improvement Association, Honolulu, USA, July 25–29, 1982.
[10] W.T. Hanbury, T. Hodgkiess, Membrane distillation: An assessment, Desalination 56 (1985) 287–297.
[11] J. Schwinge, P.R. Neal, D.E. Wiley, D.F. Fletcher, A.G. Fane, Spiral wound modules and spacers, J. Membr. Sci. 242 (2004) 129–153.
[12] K.W. Lawson, D.R. Lloyd, Membrane distillation, J. Membr. Sci. 124 (1997) 1–25.
[13] D. Winter, J. Koschikowski, M. Wieghaus, Desalination using membrane distillation: Experimental studies on full scale spiral wound modules, J. Membr. Sci. 375 (2011) 104–112.
[14] J.H. Lienhard, A. Bilton, M.A. Antar, J. Blanco, G. Zaragoza, Solar desalination, in: Annual Review of Heat Transfer, vol. 15, Begell House, New York, NY, 2012, pp. 277–347.
[15] E. Guillén-Burrieza, G. Zaragoza, S. Miralles-Cuevas, J. Blanco, Experimental evaluation of two pilot-scale membrane distillation modules used for solar desalination, J. Membr. Sci. 409–410 (2012) 264–275.
[16] E. Guillén-Burrieza, J. Blanco, G. Zaragoza, D.C. Alarcón, P. Palenzuela, M. Ibarra, W. Gernjak, Experimental analysis of an air gap membrane distillation solar desalination pilot system, J. Membr. Sci. 379 (2011) 386–396.
[17] E. Guillen-Burrieza, R. Thomas, B. Mansoor, D. Johnson, N. Hilal, H. Arafat, Effect of dry-out on the fouling of PVDF and PTFE membranes under conditions simulating intermittent seawater membrane distillation (SWMD), J. Membr. Sci. 438 (2013) 126–139.